Studies of Separation Distances in a Magnetically Driven Shock Tube with Parallel-Plate Electrodes

C. T. Chang

Association EURATOM–AEK
Danish Atomic Energy Commission Research Establishment Risø, Roskilde, Denmark

(Z. Naturforsch. **29 a**, 1838–1845 [1974]; received June 6, 1974)

The separation distances between the pressure, the luminous, the ionization and the current front in a magnetically driven shock tube were investigated under discharge conditions of constant voltage and variable pressures. In order to achieve a steady-state, one-dimensional flow- parallel-plate electrodes and a constant voltage energy source were chosen. onventional magnetic probe and piezo-electric probes were used as diagnostic tools. These were suplemented by Schlieren and holographic interferograms. Experimental results show that the observed lack of separation at low discharge pressures can be attributed to the diffusive nature of the driving current. Due to the presence of anomalous diffusion, its cause cannot be entirely explained by present theories.

I. Introduction

The shock speed attainable in conventional diaphragm type shock tubes is well known to be limited. To overcome this difficulty, the use of an electromagnetic driving force seems a logical substitute. Unfortunately, among other short-comings, the development of magnetically driven shock tubes as useful experimental devices is hampered by the lack of separation between the current sheath and the shock observed at discharge conditions of high voltage and low pressures, i. e. at conditions where high speed shocks are observed [1–10]. Since sufficient separation is important not only for the correct interpretation of the plasma state behind the shock, but is also related to the practical problem of space and time resolution of diagnostic techniques, a systematic study of its relation to the discharge conditions was undertaken.

By way of comparison, we may mention that lack of separation between the contact surface and the shock has been observed by previous investigators in diaphragm type shock tubes operating at low initial pressures ($p_1 \leqq 1$ torr) [11, 12], as well as in low density theta pinches ($N_1 \leqq 2 \times 10^{12}\mathrm{cm}^{-3}$) [13]. The cause of the observed lack of separation was attributed to the mass leakage of the compressed gas through the wall boundary layer in the former case, and to the anomalous diffusion of the current sheath in the latter case. In this respect, it would be interesting to investigate whether the observed lack of separation in the magnetically driven shock tubes could be caused by either of these effects, or whether it is due to other phenomena as reported by previous investigators [5–6].

In order to avoid unnecessary complications, it is desirable to obtain a one-dimensional flow; and to have measurements taken in regions where the flow is steady, and where the shock has a sufficient time to emerge from the current layer.

Following these considerations, we shall first present an experimental set-up designed primarily to achieve these objectives: This is followed by a description of the experimental techniques used and the results obtained. The experimentally obtained results are then analysed using current theories. Finally, after a brief discussion, a suggestion concerning future experiments is made.

Reprint requests to C. T. Chang, Danish Atomic Energy Commission, Research Establishment Risø, *DK-4000 Roskilde*, Denmark.

II. Experiments

A) Apparatus and Diagnostics

In order to achieve a steady one-dimensional flow so that the experimental results can be compared with those obtained in conventional shock tubes, a broad rail-gun with a constant voltage energy source was chosen. The electrodes consist of a pair of parallel plates, 8 cm wide, 40 cm long with a 2 cm gap; the constant voltage source is made up of a pulse net-work with a rise time of 0.4 μs and a running time of 18 μs with no crowbar facility. There is no bias field. A more detailed description of the apparatus and the experimental set-up can be found in [14].

Room temperature helium was used as the main test gas, argon was used occasionally. Most dis-

Dieses Werk wurde im Jahr 2013 vom Verlag Zeitschrift für Naturforschung in Zusammenarbeit mit der Max-Planck-Gesellschaft zur Förderung der Wissenschaften e.V. digitalisiert und unter folgender Lizenz veröffentlicht: Creative Commons Namensnennung-Keine Bearbeitung 3.0 Deutschland Lizenz.

This work has been digitalized and published in 2013 by Verlag Zeitschrift für Naturforschung in cooperation with the Max Planck Society for the Advancement of Science under a Creative Commons Attribution-NoDerivs 3.0 Germany License.

Zum 01.01.2015 ist eine Anpassung der Lizenzbedingungen (Entfall der Creative Commons Lizenzbedingung „Keine Bearbeitung") beabsichtigt, um eine Nachnutzung auch im Rahmen zukünftiger wissenschaftlicher Nutzungsformen zu ermöglichen.

On 01.01.2015 it is planned to change the License Conditions (the removal of the Creative Commons License condition "no derivative works"). This is to allow reuse in the area of future scientific usage.

charges, unless other-wisely stated, were taken at a fixed voltage of 13 kV and in the pressure range of 0.5 to 7 torr. The pressure range was limited at the lower end by the sensitivity of the differential interferometry and at the higher end by the running time of the discharge (to avoid the occurrence of a second reversed pulse). All measurements were taken in regions within the electrodes where the flow was steady, (distance travelled by the current sheet over the gap between electrodes, $x/d > 15$).

The main diagnostic tools used were a conventional magnetic probe with a linear response up to 10 MHz and a fast piezoelectric probe with a rise time of 0.2 μs. The pressure probe was of the modified Baganoff type [15, 16] and was fitted with an amplifier after the design of Hopman and Kuiper [17]. PTZ-11 was used as the sensing element with the front disc mounted about 15 cm behind a 0.4 cm diameter quartz guiding rod; silver paint, Leitsilber 204, Degussa, was used as the binding agent. The delay time of the pressure pulse was calibrated by placing the front end of the guiding rod of the probe in touch with the surface of a one cm thick PTZ-crystal (with an air gap about 1 μ thick), and by recording the arrival time of a square voltage pulse sent through the calibrating crystal.

In principle, the test time τ at a given axial position x is just the time difference between the arrival of the pressure and of the current signal, see Figure 1. Unfortunately, due to the limited space between the electrodes and the difficulty of shielding, no simultaneous readings of the two probes were made. Instead, they were correlated through the light emitted by the plasma itself. This was accomplished by focusing a beam of HeI, λ-5876 Å, light at the tip of the probe (magnetic or pressure) to the entrance slit of a monochromator, and by displaying simultaneously traces of the two signals on the screen of an oscilloscope; typical oscillograms are shown here in Figure 2. To ensure that the data obtained were reasonably representative of the average behaviour of the discharges, three separate runs were made at identical discharge conditions of voltage and filling pressure.

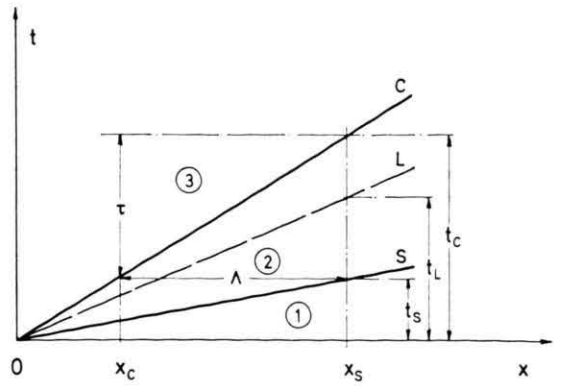

Fig. 1. Idealized trajectories of the current-sheet $\overline{OC}$, the luminous front $\overline{OL}$ and the shock $\overline{OS}$ in the $x-t$ diagram, their arrival time at a fixed location are denoted by t_C, t_L and t_S, respectively. Δ is the separation distance; $\tau = t_C - t_S$ is the test time.

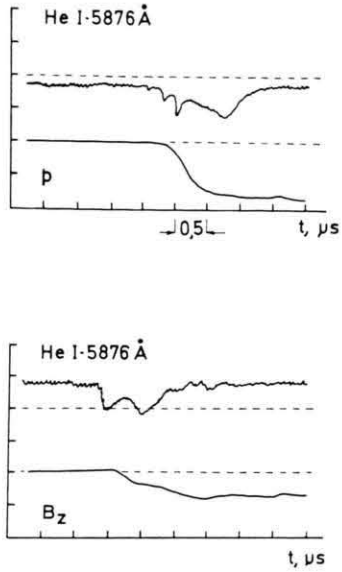

Fig. 2. Oscilloscopic traces of luminosity, pressure and the self-field B_z taken at an axial position $x = 36$ cm and discharge condition; $V_0 = 13$ kV, $p_1 = 1$ torr. The onset time of the pressure pulse in the upper figure is 0.2 μs ahead of the light.

In order to avoid possible disturbances introduced during the measurements, and also to serve as a separate means of checking the results obtained by probes, smear pictures of Schlieren, or differential, interferograms were taken at identical discharge conditions. The technique involved and the set-up used were quite similar to those of previous investigators [18–20]. The light source used was a pulsed, high pressure mercury lamp, Osram type HBO-100. To reduce the intensity of the plasma light, narrow band filters (λ-5461 and λ-4358 Å) were used. Typical smear pictures are shown in Figure 3 *. They were supplemented by time-lapsed holographic interferograms, taken in the pressure range of 0.2 – 5 torr. The set-up used was similar to the one used in the plasma focus experiments [21]; a Q-switched ruby laser was used as the light source. Examples are shown here in Figure 4.

Finally, an estimate of the average electron temperature in the current layer was made from the line

* Figure 3 and 4 on page 1842 a, b.

intensity-ratio He II-4686/He I-5876, and the average electron number density was obtained from the half-width of these lines [22].

B) Results

1) Variation of the Test Time τ with Respect to the Steady-state, Current-sheet Speed $\hat{u}$

In Fig. 5, the time difference $\Delta_P = t_s - t_L$, between the arrival of the pressure front and of the luminous front (λ-5876 Å), and similarly the time difference $\Delta_B = t_c - t_L$, between the arrival of the

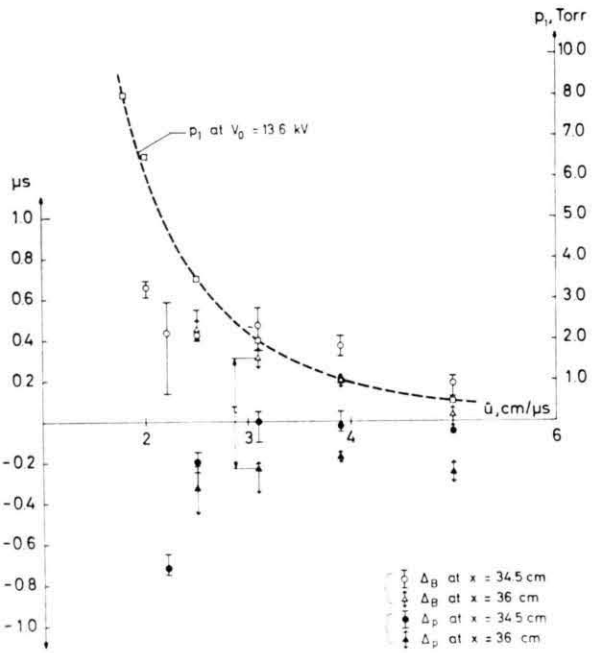

Fig. 5. Difference in the arrival time of the various fronts at a given location x with respects to the steady state current-sheet speed $\hat{u}$. $\Delta_P = t_s - t_L$ is the time difference between the arrival of the pressure and of the luminous front; $\Delta_B = t_c - t_L$ is the time difference between the arrival of the current and of the luminous front. The dashed curve gives the average discharge pressure p_1 at the corresponding current-sheet speed $\hat{u}$.

current front and the luminous front, at a given axial position x, are plotted against the steady state current-sheet speed $\hat{u}$. For reference purposes in the same figure we have also shown the average discharge pressure p_1, corresponding to the indicated current-sheet speed, $\hat{u}$, at the given discharge voltage of 13 kV.

From the figure one observes that at an axial position x = 34.5 am, a time difference Δ_P between the arrival of the two fronts is noticeable only for a current-sheet having speeds $\hat{u}$ below 3 cm/μs, or at the given discharge voltage of 13 kV only for pressures above 2 torr. The general trend is that at a fixed axial position x, as the current-sheet speed $\hat{u}$ increases, both time differences Δ_P and Δ_B tend to decrease; and at the same current-sheet speed $\hat{u}$, as the observing position x increases, Δ_P increases also, but the opposite is observed for Δ_B.

From these results the test time $\tau = \Delta_B - \Delta_P$ is derived and is plotted as the dimensionless ratio τ/t_c versus the steady-state current-sheet speed $\hat{u}$ in Fig. 6; where t_c, as shown in Fig. 1, is the arrival time of the current-sheet at the given axial position x.

2) Interpretation of the Smear Differential Interferogram Records

From the information gathered about Δ_B, and in view of the writing speed of the streak camera, 0.98 mm/μs, we shall expect a practical coincidence of the luminous front and the current-sheet in the smear photographs. An examination of the photographic records, e. g. Fig. 3, shows that this is the case, provided that we interpret an upward fringe shift in the smear differential-interferograms as a positive increase of the gradient of the electron number density, and the current-sheet as a region where the number density of electrons is at its maximum, (i. e. the fringe pattern in the pictures has the shape of a letter N). As a result, we shall interpret the first upward fringe shift in these photographs as an indication of the initiation of ionization. From previous data of Δ_P, and within the limitation of the diagnostic means used, we infer that the ionization and the pressure front are almost indistinguishable in most cases.

These pictures further show that the three fonts of ionization, current and luminosity almost coincide in the lower pressure case; whereas the ionization front definitely leads the current-sheet in the higher pressure case.

The general features of the differential-interferograms are thus in agreement with those obtained from the probe data.

3) Holographic Interferometry

The refractivity $(n-1)_\lambda$ of a helium plasma in the visible region can be divided approximately in two parts; a non-dispersive part due to the particle concentration of "atoms" N_a (He I + He II) and a

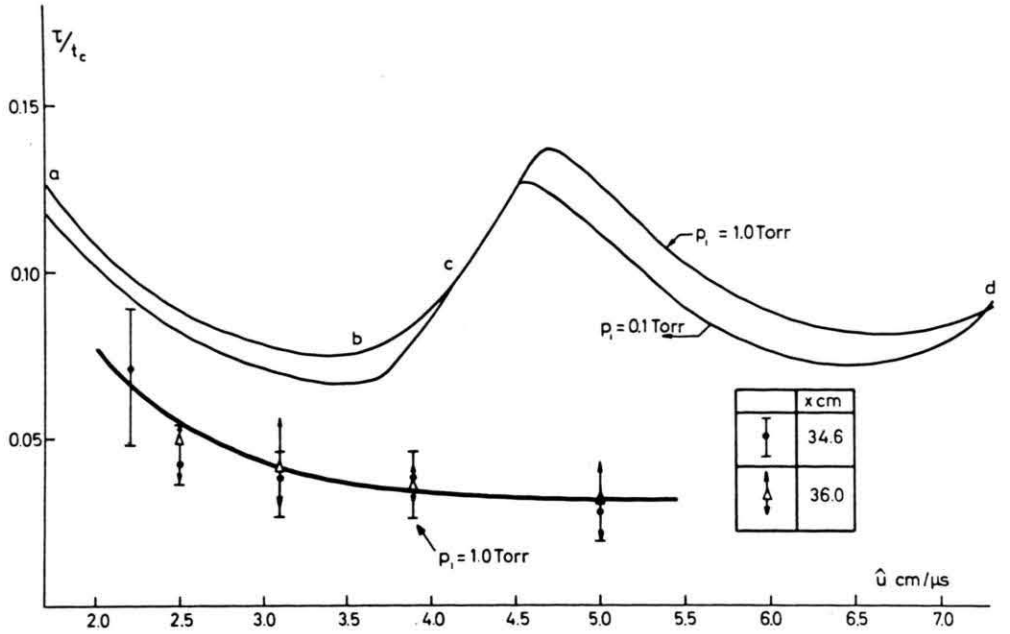

Fig. 6. τ/t_c, ratio of the test time and the time of arrival of the current-sheet at the axial position x vs. the steady-state current-sheed speed $\hat{u}$. The two upper curves are drawn according to the theoretical calculations by taking the ionization effect into consideration; the lower curve is drawn according to the trend indicated by the experimental data.

dispersive part due to the electron concentration, N_e, thus

$$(n-1)_\lambda = 0.13\times10^{-23}\,N_a(\mathrm{cm}^{-3}) - 4.46\times10^{-14}\,\lambda^2(\mathrm{cm}^2)\;N_e(\mathrm{cm}^{-3})\,. \quad (1)$$

One observes at a given wavelength λ that the refractive index changes its sign from positive to negative once the degree of ionization becomes noticeable. At the wavelength $\lambda = 6943$ Å of the ruby laser, this occurs when $N_e/N_a > 0.006$. In an idealized shock, elastic collisional processes usually occur at a much faster rate than inelastic processes. This implies that when direct interferograms are taken, as one proceeds downstream from the shock front, the fringes should first shift towards one direction and then towards the opposite direction.

As shown in Fig. 4, the results as indicated by the holographic interferograms are contrary to expectations, but agree with those of the smear differential-interferograms, i. e. there is a coincidence between the pressure and the ionization front. These holograms also showed that the current layer, as indicated by the fringe shift, is thinner in the low pressure case (~ 3 cm) than in the higher pressure case (more than 5 cm).

4) Planarity of the Shock

Records of the holographic interferograms further showed that within the pressure range of $1-5$ torr, the shock front appears to be reasonably flat. Generally speaking, at the given discharge voltage of 13 kV, a better planarity is observed at a higher discharge pressure.

5) Average Plasma State in the Current Layer

At the discharge condition of 13 kV and 0.5 torr, the electron temperature T_e estimated from the line intensity ratio of He II-4686/He I-5876, averaged over a time interval of 1 μsec, is about 3.5 eV. Due to the uncertainty of the plasma opacity towards the He II resonance line (λ-303 Å)[23], an error of ± 0.5 eV could be expected. The corresponding number density, N_e, estimated from the half width of He I-5876 is around 1.6×10^{17}, which is in reasonable agreement with the result deduced from the holographic interferograms. One observes that the measured values of T_e and N_e are about the same as the calculated values of the post-shock equilibrium state indicated in Table 1.

Table 1. Minimum time, t^*, required for separation at a discharge voltage of 13 kV in helium, according to classic diffusion.

P_1 torr	W_s cm μs	η	T_e eV	$\mu\sigma$ MKS unit	$\dot{\delta}_1$ cm/μs	t^* μs
0.2	7	13	4.8	$9.17\times10^{-3}(Z_i=2)$	1.04	3.73
				$1.83\times10^{-2}(Z_i=1)$	0.739	1.89
0.5	5	8	4	1.40×10^{-2}	0.845	1.82
1	4	13	2	6.90×10^{-3}	1.20	15

Note: The two values listed in the last three columns ta the discharge pressure $p_1=0.2$ torr are due to the dependence of the conductivity σ on the ionic charge.

III. Theoretical Consideration

As a point of reference, the ideal case will be treated first; deviations from this due to various physical effects will be discussed subsequently.

1) The Ideal Case

Assuming the current-sheet is accelerated instantaneously to the steady state, the trajectories of the current-sheet and the shock can be represented as the two divergent lines OC and OS in the $x-t$ plane, see Figure 1. From the law of conservation of mass, one can relate the separation distance, Δ to the location x_s where the shock is first detected, or the test time τ to the time of arrival of the current-sheet t_c at x_s through the compression ratio $\eta(\equiv\varrho_2/\varrho_1)$ by

$$\Delta=x_s/\eta \quad \text{and} \quad \tau/t_c=1/\eta\,. \tag{2}$$

For an idealized monatomic gas, devoid of internal degrees of freedom, the compression ratio η equals four; thus $\tau/t_c=0.25$.

2) The Effect of Ionization

Calculations based on statistical mechanics showed that the compression ratio η has two maxima corresponding to the two stages of ionization of helium at a shock speed $w_s=4$ and 7.5 cm/μs [24]. From Eq. (2) it follows that τ/t_c has two minima at the steady state current sheet speed $\hat{u}=3.5$ and 6.5 cm/μs, respectively. A comparison between the experimental trend and the theoretical result showes that although ionization might play some role for low speed shocks, it certainly cannot be the dominating effect for high speed shocks.

3) The Effects of Mass Leakage in the Compressed Region

a) The Effect of Viscous Boundary Layer at the Wall

Experiments performed by previous investigators in conventional shock tubes operating at low initial pressure ($\sim$1 torr) showed, contrary to expectations, that as the length of the expansion chamber is successively extended, the separation distance tends towards a limiting value, and remains constant with the distance travelled by the shock thereafter. The maximum test time τ_m, corresponding to the limiting separation distance, is shown to vary linearly with the initial pressure. The effect was attributed to the mass leakage through the boundary layer at the wall [11, 12].

The importance of the boundary layer effect depends on the ratio between the displacement thickness and the hydraulic diameter [25]; or, in our case, it depends on the ratio of the displacement thickness and the gap between the electrodes. Detailed calculation showed that this ratio cannot be more than 0.2 [26]. Furthermore, differential interferograms indicated that the thickness of the boundary layer does not seem to exceed 1 mm. From these considerations, we conclude that the observed lack of separation between the current-sheet and the shock cannot be explained by the boundary layer effect.

b) The Effect of a Perforated Current-Sheet

As an alternative leakage mechanism, one may imagine that due to low ionization efficiency or charge transfer processes there is a considerable mass leakage through the current-sheet itself. Assuming that the matter leaked through the sheet is in the unionized state and treating the current-sheet as a thin perforated screen, a simplified calculation shows that such a model could cause the sheet to move at a speed comparable to that of the shock [27]. The direct application of this model towards the interpretation of our experimental results, however, is limited. This is because, according to the model, small separations are particularly to be expected for current-sheets moving faster than the ideal snowplough; whereas the measured current-sheet speeds, due to the diffusion of the driving current, are considerably lower than those predicted by the ideal snowplough model [28].

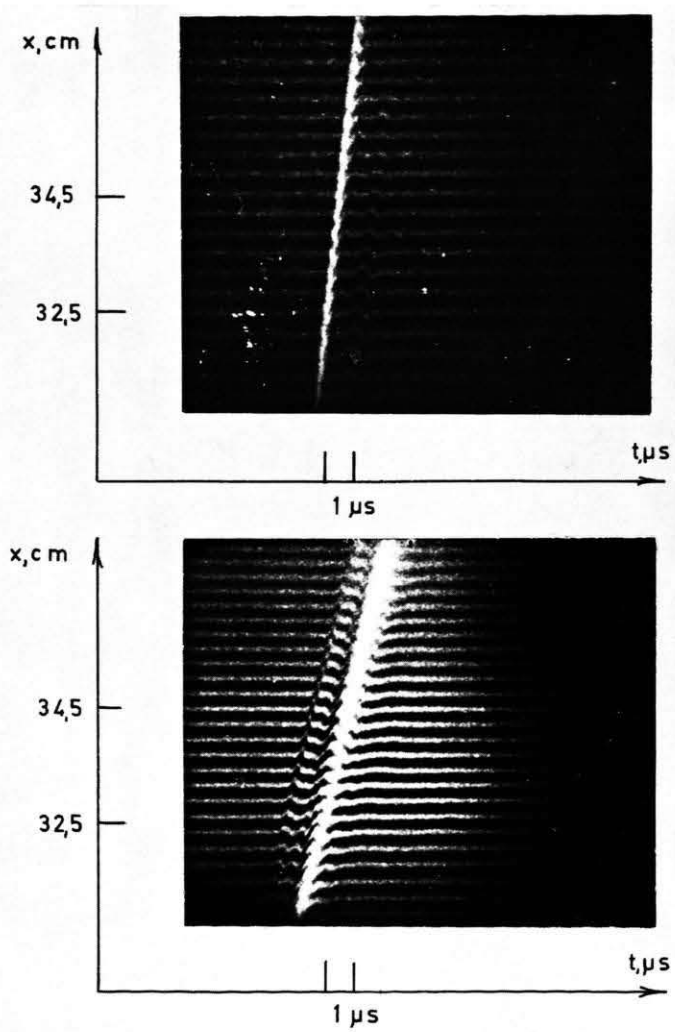

Fig. 3. Smear photographs of the differential-interferograms with the superimposed plasma light of He I-5876 Å. Light source, high pressure mercury lamp with a narrow band filter. The upper picture is taken at a discharge voltage $V_0 =$ 13 kV, an initial pressure $p_1 = 1$ torr and λ-5461 Å; the lower picture is taken at the same discharge voltage but at a pressure $p_1 = 5$ torr and at λ-4358 Å.

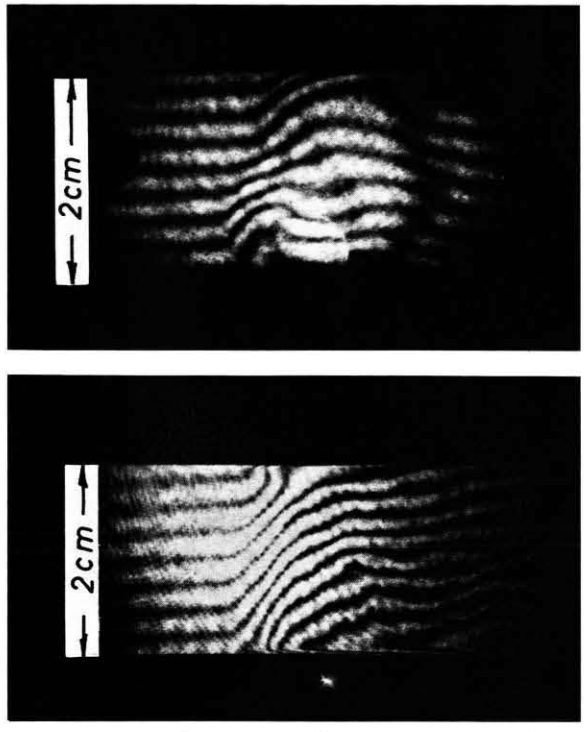

Fig. 4. Time-lapsed holographic interferograms taken at an axial position $x=36$ cm with a Q-switched ruby laser. Discharge conditions: upper picture, $V_0=13$ kV, $p_1=0.2$ torr; lower picture, $V_0=13$ kV, $p_1=5$ torr. The upward fringe shifts indicate an increase of the electron refractive index.

4) The Effect of Finite Electrical Conducivity

a) The Skin-depth Criterion

In an idealized magnetically driven shock tube, the driving current is assumed to be confined in a thin sheet; or equivalently, the conductivity σ of the plasma is infinite. In reality, due to the finite conductivity, the current will spread in time. From the random-walk concept, one expects the thickness of the layer, δ, to grow at a rate proportional to $(t)^{-\frac{1}{2}}$. Consequently, if the shock moves at a constant speed, it should eventually separate from the current layer. However, the operational duration of most magnetically driven shock tubes is rather short ($\sim 10\,\mu$s), and thus it is quite conceivable that due to the diffusion of the current layer the shock may have insufficient time to emerge from the current layer. By equating the growth rate of the current layer to that of the separation distance, the minimum t^* required for the separation to occur can be estimated thus

$$t^* = (\dot{\delta}_1 \eta / w_s)^2 , \tag{3}$$

where

$$\dot{\delta}_1 = \theta / 2\,(\mu\,\sigma)^{1/2} , \tag{4}$$

and θ is a numerical constant depending on the detail of the diffusion process, σ is the electrical conductivity, and μ is the magnetic permeability.

Taking the observed current-sheet speed $\hat{u}$ as the shock speed W_s, and assuming the existence of a post-shock equilibrium state, the compression ratio, η, and the electron temperature, T_e, are inferred from the work of Fucks and Artmann [24]. Using these data and Spitzer's formula [29], we have calculated the conductivity σ corresponding to a given discharge of 13 kV and initial pressures of 0.2, 0.5 and 1 torr. Taking $\theta = 2$ [20], the minimum t^* is obtained from Eq. (3) and is shown in Table 1 along with other relevant parameters. Actually $W_s \geqq \hat{u}$, and the numerical value of the constant θ, are rather uncertain, t^* could differ from the values given in the table, but this will not invalid the indicated trend, namely that if the skin-depth effect is important, a better separation is expected to occur at a higher current-sheet speed. This has not been observed in our experiments.

The above result, however, is based on the concept that the field diffuses classically. Reports from recent experiments conducted in low density theta pinches have shown that due to the presence of anomalous diffusion, the current layer grows linearly in time [13]. Since the shock produced in those cases was collision-free, while ours was collision-dominated, a direct comparison between the two cases is not possible. Nevertheless, as shown in Fig. 7, the current layer thickness $\delta_{0.8}$ (corresponding to eighty per cent of the total current delivered) derived from the magnetic probe data indicated a growth faster than that given by the parabolic law. The presence of some kind of anomalous diffusion under our experimental conditions is evident.

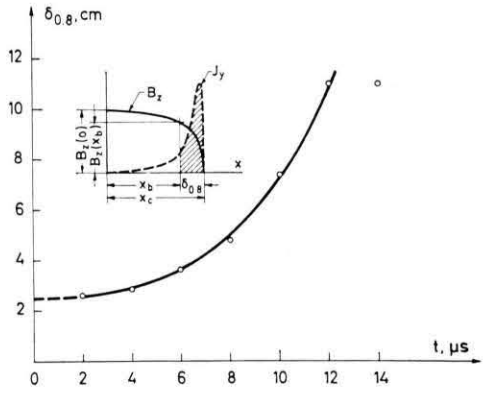

Fig. 7. Variation of $\delta_{0.8}$ with respect to the time. $\delta_{0.8} = x_c - x_b$ is the current layer thickness containing 80% of the total current delivered to the electrodes. x_c is the leading edge of the layer where $B_z(x_c) = 0$; x_b is the abscissa of the curve $B_z(x)$ where $B_z(x_b) = 0..8\,B_z(0)$. A one-dimensional current density distribution $J_y(x)$ is assumed. Discharge condition, 13 kV. 10 torr in He.

b) Emergence of the Shock from the Current Layer

The previous treatment, however, implicity assumes that (a) after the breakdown, the current flows in a thin layer, i.e. $\delta(0) = 0$; (b) the conductivity σ is constant; (c) a shock has already formed ahead of the current-sheet, i.e. the shock formation time $t_f < t^*$. In experiments without preionization, the current formed after the breakdown is distributed in a layer of finite thickness. As the layer advances along the electrodes, it compresses and ionizes the gas upstream and leaves an expansion region downstream. This lowers the conductivity in time and causes a growing wake trailing behind [28]. As a result, the driving force field changes from a localized mode to a diffusive mode. The effect is further argumented at low discharge pres-

sures due to the reduction of the conductivity through the Hall effect.

According to Hoffman [31] and Steinolfson [32], when a medium is compressed by a distributive force (e. g. the current layer) moving at a constant speed, the formation of a shock depends upon the speed of the force field with respect to the acoustic speed of the medium at rest. For a current layer moving at supersonic speed, as in our experiments, a shock is formed within the layer; near its rear edge for a fast current layer and near its front edge for a slow one. When a diffusion effect is also present, the controlling parameters are the magnetic Reynolds number of th current layer and its Mach number relative to the gas at rest. The shock will form sooner for a current layer having a high magnetic Reynolds number and a low Mach number; lowering the Mach number, however, is more influential in causing the shock to form at the front of the current layer than raising the magnetic Reynolds number. This seems to be consistent with our experimental results.

IV. Summary and Discussion

From the information presented previously, we may summarize our experimental results as follows:

i) Qualitatively our results are in agreement with those obtained by previous investigators [1–9]; a sufficient separation between the shock and the current-sheet or the luminous front is observed only at discharge conditions where slow current-sheets are produced.

ii) A longer test time is observed for a longer travel of the current-sheet provided that the second discharge is not initiated.

iii) The measured test time τ is considerably lower than those calculated on the basis of the conservation of mass and the effect of ionization;

iv) Within the limitation imposed by experimental techniques and in the range of discharge voltage and pressure investigated, the pressure front and the ionization front are almost indistinguishable; the luminous front tends to lead the current-sheet for slow current-sheets but tends to merge with the sheet for fast current-sheets.

Among various phenomena considered, neither the effect of thermal ionization nor the broadening of the current layer due to classic field-diffusion can explain the observed result. In view of the fact that mass leakage through the wall boundary layer is definitely without importance, we conclude that, although the observed lack of separation seems to occur at the same conditions of low initial pressure as observed in diaphragm-type shock tubes, their causes are quite different.

On the other hand, mass leakage through the sheet itself could give a possible explanation. However, since the mass leaked through the sheet seems to be in the ionized state, its net result is equivalent to that caused by a diffusive current layer. According to the work of Steinoldson [32], for a given force field moving at a constant speed, the shock tends to form further behind the force field either as the speed of the force field is increased, or as the strength of the driving force is reduced. In a magnetically driven shock tube, the driving force can be writen as $\frac{1}{2} L_1 \hat{I}^2$, where L_1 is the inductance gradient per unit length of the electrodes and $\hat{I}$ is the steady-state current delivered to the shock tube. When discharges are running at constant voltage, as the filling pressure p_1 is reduced, the speed of the current sheet increases; but the driving force is reduced on account of the lowering of the inductance gradient L_1 [28], as well as due to the reduction of the driving current $\hat{I}$, see Figure 8. Our experimental results, therefore, seem to be in qualitative agrement with the theoretical prediction of a distributive force. However, in view of the fact that the current layer appears to be thicker at higher than at lower discharge pressures, and grows at a rate faster than that given by the parabolic law, we feel that while the lack of separation in our experiments is due definitely to the diffusive nature of the force field, it is still difficult to explain the observed effect entirely on the basis of present theories.

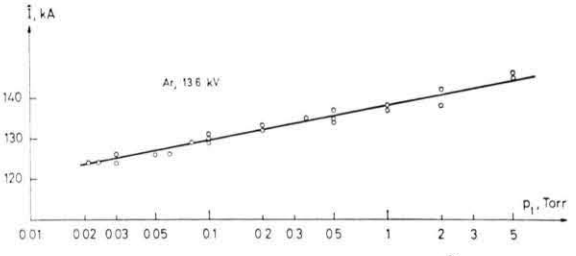

Fig. 8. Variation of the steady- state current $\hat{I}$ with respect to the discharge pressure p_1 at a fixed discharge voltage $V_0 = 13.6$ kV.

To clarify these questions, a detailed study of the trajectories of the pressure and of the current front,

as well as the growth of the current layer under different discharge conditions, is much desired. In principle, this could be done experimentally by taking smear interferograms at two wavelengths simultaneously. Unfortunately, due to the lack of a suitable light source and proper recording devices, and also as the result of a reorientation of our research programme, this was not possible in the course of our experiments.

As a final remark, we may mention that sufficient separation between the shock and the current-sheet has been reported on several occasions in experiments dealing with M.H.D. shocks [33], collisionless shocks [13, 34–39], as wel as gasionizing shocks [39]. However, in the first two cases, preionization and a bias field were used, while in the last case a bias field was always present. Our results, therefore, should be viewed rather as complementary than contradictory to these.

Acknowledgements

The differential-interferograms were taken by M. Popović. B. Hurup Hansen constructed the pressure probe and participated in all phases of the experiment.

[1] C. T. Chang, Phys. Fluids **4**, 1085 [1961].
[2] P. Jeanmarie, H. Klingenberg, and H. Reichenbach, Z. Naturforsch. **18 a**, 318 [1963].
[3] W. Fucks and R. Teenhaus, Z. Physik **177**, 269 [1964].
[4] Brinkschulte and H. Muntenbruch, Z. Naturforsch. **20 a**, 196 [1965].
[5] G. C. Vlasses, Phys. Fluids **10**, 2351 [1967].
[6] F. Y. Sorrell, Phys. Fluids **11**, 993 [1968].
[7] F. Y. Sorrell, Phys. Fluids **12**, 1218 [1969].
[8] A. L. Hoffman, Phys. Fluids **12**, 1426 [1969].
[9] A. Belozerov, Institute for Aerospace Studies, University of Toronto, UTIAS Report No. 131 [1968].
[10] D. C. Wisler and Y. Nagakawa, Phys. Fluids **15**, 1948 [1972].
[11] R. E. Duff, Phys. Fluids **2**, 207 [1969].
[12] A. Roshko, Phys. Fluids **3**, 835 [1960].
[13] M. Keilhacker, M. Kornherr, G. Maret, H. Niedermeyer, and K. H. Steuer, Proc. 6th Europ. Conf. Controlled Fusion and Plasma Physics Moscow 1973, Vol. 1, p. 307.
[14] M. Popović, Danish AEC Research Establishment, Rosø Report No. 206 (1969).
[15] D. Baganoff, Rev. Sci. Instrum. **35**, 288 [1964].
[16] W. Katsaros, Institut für Plasmaphysik, Garching, Report IPP 1/46 (1946).
[17] K. H. Finken, Institut für Plasmaphysik, KFA Jülich, Report Jül.-607-pp (1969).
[18] H. Oertel, Sixth Int. Congress on High-Speed Photograph, Hague/Scheverringen, (Netherlands 1962), paper No. XII-F.
[19] A. Heiss, Institut für Plasmaphysik, Garching, Report IPP 1/25 (1964).
[20] W. Zimmerman, Institut für Plasmaphysik, Garching, Report IPP 3/57 (1967).
[21] T. D. Butler, I. Hennès, F. C. Jahoda, J. Marshall, and R. L. Morse, Phys. Fluids **12**, 1904 [1969].
[22] H. R. Griem, Plasma Spectroscopy, McGraw-Hill, New York 1964, chapters 13 and 14.
[23] R. Mewe, Brit. J. App. Phys. **18**, 107 [1967].
[24] W. Fucks and J. Artmann, Z. Physik **172**, 118 [1963].
[25] H. Mirels in "Shock Tube Research", Proc. of the 8th Int. Shock Tube Symp., J. L. Stolley, A. G. Gaydon and R. R. Owen, eds., Chapman and Hall, London 1971, paper No. 6.
[26] C. T. Chang, Risø Report (to be published).
[27] C. T. Chang, Plasma Physics **15**, 1265 [1973].
[28] C. T. Chang, M. Popović, and U. Korsbech, Plasma Physics **12**, 751 [1970].
[29] L. Spitzer, Jr., Physics of Fully Ionized Gases, Interscience, New York and London 1962, chapter 5.
[30] T. J. Falk and D. L. Turcotte, Phys. Fluids **5**, 1288 [1962].
[31] A. M. Hoffman, J. Plasma Phys. **1**, 193 [1967].
[32] R. S. Steinolfson, A.I.A.A. J. **11**, 1201 [1973].
[33] W. R. Bell, A. E. Bishop, H. J. Crawley, G. D. Edmonds, J. W. M. Paul, and J. Sheffield, Proc. Inst. Elec. Engrs. London **113**, 2099 [1966].
[34] M. Camac, A. R. Kantrowitz, M. M. Litvak, R. M. Patrick, and H. E. Petschek, Nucl. Fusion Suppl. Pt **2**, 423 [1962].
[35] J. W. M. Paul, L. S. Holmes, M. J. Parkinson, and J. Sheffield, Nature London **208**, 133 [1965].
[36] R. Chodura, M. Keilhacker, K. Kornherr, and H. Niedermeyer in "Plasma Physics and Controlled Nuclear Fusion Research" 1968, IAEA, Vienna 1969, vol. 1, p. 81.
[37] S. E. Segre and M. Martone, Plasma Physics **13**, 113 [1971].
[38] E. Hintz in "Methods of Experimental Physics" vol. 9, part A, Plasma Physics, H. R. Griem and R. H. Lovberg, eds., Academic Press, New York and London 1970, chapter 6.
[39] Y. G. Chen, C. K. Chu, R. A. Gross, E. Halmoy, P. Moriette, and S. Schneider in "Plasma Physics and Controlled Nuclear Fusion Research" 1971, IAEA, Vienna 1971, vol. III, p. 241.